

Substructure considerations rule out dark matter interpretation of *Fermi* Galactic Center excess

Hamish A. Clark,^{1,*} Pat Scott,² Roberto Trotta,^{2,3} and Geraint F. Lewis¹

¹*Sydney Institute for Astronomy, School of Physics A28,
The University of Sydney, NSW 2006, Australia*

²*Department of Physics, Imperial College London,*

Blackett Laboratory, Prince Consort Road, London SW7 2AZ, UK

³*Data Science Institute, William Penney Laboratory, Imperial College London, London SW7 2AZ*

(Dated: December 26, 2022)

An excess of gamma rays has been identified at the center of the Milky Way, and annihilation of dark matter has been posited as a potential source. This hypothesis faces significant challenges: difficulty characterizing astrophysical backgrounds, the need for a non-trivial adiabatic contraction of the inner part of the Milky Way’s dark matter halo, and recent observations of photon clustering, which suggest that the majority of the excess is due to unresolved point sources. Here we point out that the point-like nature of the emission rules out the dark matter interpretation of the excess entirely. Attempting to model the emission with dark matter point sources either worsens the problem with the inner slope, requires an unrealistically large minihalo fraction toward the Galactic Center, or overproduces the observed emission at higher latitudes.

Introduction.— An excess of high-energy gamma rays has been observed toward the Galactic Center (GC) by the *Fermi* Large Area Telescope (*Fermi*-LAT; [1]). This excess is not easily explained by known astrophysical sources. It peaks at energies of ~ 2 GeV, appears spherically distributed, extends up to 1.5 kpc from the GC, and falls steeply with distance from the GC, exhibiting a profile that goes as $r^{-\Gamma}$, $\Gamma \sim 2.2$ – 2.8 [2–4]. Proposed explanations include cosmic ray injection [5–7], a population of unresolved millisecond pulsars [8–10], or the self-annihilation of dark matter (DM) within the Milky Way’s halo [11–13].

Among these interpretations, DM self-annihilation is of particular interest, as it would allow a characterization of the particle nature of DM. Should it annihilate, DM may be expected to produce observable radiation from the direction of the GC. For particular annihilation final states, this explanation has been found to be an excellent fit to all of the the spectral and morphological properties of the observed excess [13, 14]. However, recent analyses of *Fermi*-LAT photon map statistics [15, 16] have suggested that the vast majority of the excess originates from unresolved point sources, providing weight to the millisecond pulsar hypothesis.

The DM halo of the Milky Way is expected to contain a population of subhalos. The exact nature and abundance of the substructure is unknown. However, cold dark matter simulations predict the existence of small-scale structure [17], which should theoretically exist right down to the DM free-streaming scale. If DM annihilates, these substructures would provide a significant boost to the observed annihilation rate [18–20], contributing substantially to the overall gamma-ray emission observed from the Galactic Center.

In this Letter we investigate the possibility that the unresolved point sources identified by Bartels *et al.* [15]

and Lee *et al.* [16] may be small-scale DM halos. This scenario could potentially rescue the DM interpretation of the excess, by remaining compatible with observations of photon clustering that indicate a point-source origin for the emission. In order to determine the viability of such a scenario, we investigate the morphology and implied photon statistics of this boosted signal, using *Fermi*-LAT observations to constrain the model parameters. For all substructure cases that we consider, we find that the signal can be explained by the presence of DM substructure only if the inner slope of the Milky Way’s DM halo is drastically steepened by adiabatic contraction, or if the concentration of subhalos increases substantially toward the Galactic Center. The parameter values that this requires are so different to results obtained from state-of-the-art numerical simulations that we conclude substructure considerations rule out a dark matter interpretation of the excess.

Structure & Substructure.— We model the density profile of the smooth DM halo of the Milky Way with the generalized Navarro-Frenk-White (NFW) profile [21, 22],

$$\rho(r) = \frac{\rho_0}{\left(\frac{r}{r_s}\right)^\gamma \left(1 + \frac{r}{r_s}\right)^{3-\gamma}}, \quad (1)$$

where ρ_0 is fixed by the local DM density at the position of the Sun ($\rho_\chi = 0.3$ GeV cm⁻³, at $r_\odot = 8$ kpc), $r_s = 20$ kpc is the scale radius of the Milky Way, and γ is the inner slope of the halo.

Given the difference in their typical formation histories, low-mass substructures have different characteristics to their large-scale counterparts. As such, the properties of dark matter substructure must be decoupled from those of the Galactic halo. In what follows, we consider annihilation within two different models of substructure: NFW subhalos, and ultracompact minihalos (UCMHs).

In order to quantify the properties of the substructure in a simple manner, we make the assumption that all subhalos are of the same mass, M_h . Given that the spatial distribution of the properties of low-mass subhalos are poorly constrained, this is the simplest assumption available. For all the scenarios that we consider here, we have checked that changing this assumption to incorporate more complex mass distributions (a uniform or power-law mass distribution) does not significantly alter our results.

NFW Subhalos.— N-body simulations predict small-scale substructure down to their smallest resolvable scale, with densities that appear to follow the NFW profile [17, 23, 24]. We model NFW substructure with this density profile, parameterized by the inner slope α , as

$$\rho_h(r) = \frac{\delta_c \rho_c}{\left(\frac{r}{r_s}\right)^\alpha \left(1 + \frac{r}{r_s}\right)^{3-\alpha}}, \quad (2)$$

where

$$\delta_c = \frac{200}{3} \frac{c_{200}^3}{\Phi(c_{200})}, \quad (3)$$

$$\Phi(x) = \frac{x^{3-\alpha}}{3-\alpha} {}_2F_1(3-\alpha, 3-\alpha; 4-\alpha; -x), \quad (4)$$

and ${}_2F_1(a, b; c; d)$ is the Gaussian hypergeometric function, $\rho_c = 3H_0^2/8\pi G$ is the critical density of the Universe today, H_0 is the present-day value of the Hubble constant, G is the gravitational constant, and c_{200} is the halo concentration parameter, taken as a function of subhalo mass following Correa *et al.* [25]. The scale radius may be calculated as a function of the halo mass by

$$r_s = \left(\frac{3M_h}{800\pi\rho_c c_{200}^3}\right)^{1/3}. \quad (5)$$

Ultracompact Minihalos.— Large amplitude density fluctuations in the early Universe ($10^{-3} \lesssim \delta \lesssim 0.3$) lead to an increased production of dense small-scale structures, known as ultracompact minihalos (UCMHs; [26–29]). Should DM annihilate, these would be expected to be strong sources of annihilation products [27], and therefore strong probes of small-scale cosmology [30–33]. In what follows, we consider UCMH substructure as summarized in [31]. The density profile of a UCMH at redshift $z = 0$ may be calculated as

$$\rho_h(r) = \kappa r^{-9/4}, \quad (6)$$

where

$$\kappa \equiv \frac{3f_\chi M_h}{16\pi R_h^{3/4}}, \quad (7)$$

and f_χ is the fraction of matter that is cold dark matter, M_h is the mass of the halo, and R_h is the radius of the

halo,

$$\frac{R_h}{\text{pc}} = 1.73 \left(\frac{M_h}{M_\odot}\right)^{1/3}. \quad (8)$$

UCMH density profiles are expected to soften in the innermost regions, at radii smaller than some core radius

$$r_c = \max(r_{\min}, r_{\text{cut}}). \quad (9)$$

Here r_c is the greater of the effective annihilation radius r_{cut}

$$r_{\text{cut}} = (\kappa \Delta t \langle \sigma v \rangle / m_\chi)^{4/9}, \quad (10)$$

given as the extent of the inner region expected to have annihilated away over the UCMH lifetime Δt (which we take to be the time since equality), and the angular momentum radius r_{\min} ,

$$r_{\min} \approx 2.9 \times 10^{-7} R_h \left(\frac{1000}{z_c + 1}\right)^{2.43} \left(\frac{M_h}{M_\odot}\right)^{-0.06}, \quad (11)$$

which is the inner radius at which the radial infall approximation becomes inappropriate.

Flux from Dark Matter Self-Annihilation.— The presence of substructure within the Galaxy substantially increases the rate at which DM annihilates. The addition of even a small population of overdensities can boost annihilation by orders of magnitude, depending upon the nature and prevalence of the subhalos. Here we calculate the spatially-averaged total flux expected to be produced by a substructure population embedded within the smooth DM halo of the Milky Way.

For a spherically symmetric halo at a distance $d > R_h$ the total gamma-ray flux due to DM annihilation, differential in energy, is given by

$$\mathcal{F}_h(d, E) = \sum_k \frac{dN_k}{dE} \frac{\langle \sigma_k v \rangle}{2d^2 m_\chi^2} \int_0^{R_h} \rho_h^2(r) r^2 dr, \quad (12)$$

where $\rho_h(r)$ is the DM density at a distance r from the center of the halo, m_χ is the DM particle mass, R_h is the maximum radius of the halo, and dN_k/dE and $\langle \sigma_k v \rangle$ are the differential photon yield and cross section from the k th annihilation channel, respectively.

Likewise, the flux per unit volume from the smooth DM component with local density ρ_χ at a distance d may be found as

$$\mathcal{F}_{\text{smooth}}(d, E) = \sum_k \frac{dN_k}{dE} \frac{\langle \sigma_k v \rangle}{2d^2 m_\chi^2} [(1-f)\rho_\chi]^2, \quad (13)$$

where f is the fraction of DM that is contained within substructure, such that the DM density of the smooth component is reduced by a factor of $1-f$.

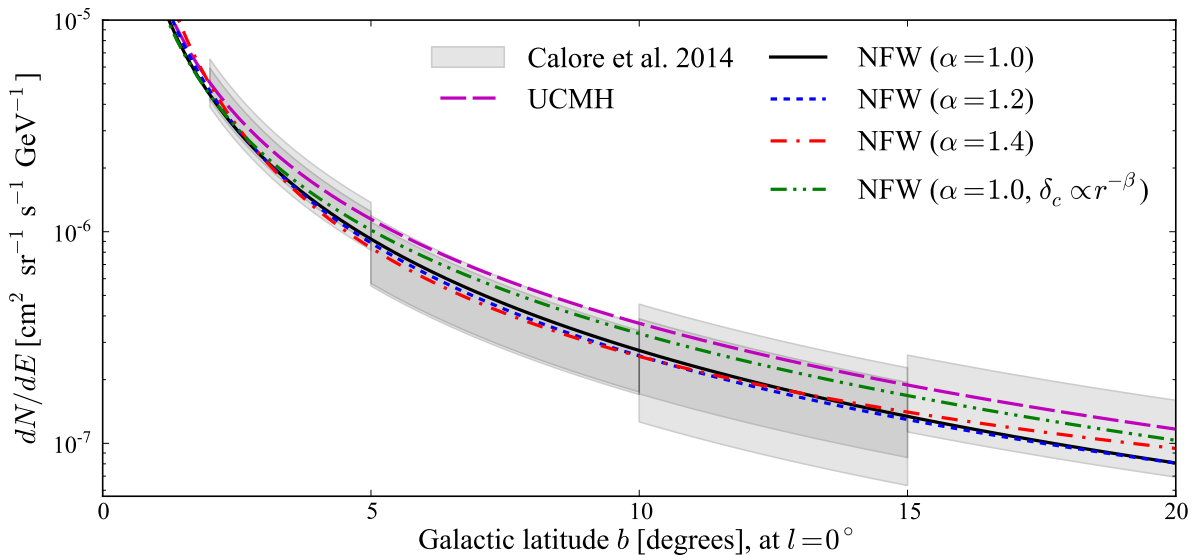


FIG. 1. Radial differential flux profile of the *Fermi* gamma ray excess as at 2 GeV, with posterior mean DM annihilation flux profiles for different substructure models: ultracompact minihalos (UCMH), and NFW subhalos with inner slopes $\alpha = 1.0, 1.2$ and 1.4 . The flux extracted within each ROI by Calore *et al.* [14] are shown as 68% confidence level shaded bands, plotted as $\mathcal{F} \propto r^{-2.7}$ within each ROI to guide the eye, and including both statistical and systematic errors. Overlapping regions correspond to the north and south regions of the sky. Note that for clarity, we do not plot the two additional extended ROIs at $l \neq 0^\circ$ included in our fit.

Additionally, there is a contribution from the annihilation of DM particles within the smooth component with those within the overdense region of the subhalo:

$$\mathcal{F}_{\text{cross}}(d, E) = \sum_k \frac{dN_k}{dE} \frac{\langle \sigma_k v \rangle}{2d^2 m_\chi^2} \int_0^{R_h} 2(1-f) \rho_\chi \rho_h(r) r^2 dr. \quad (14)$$

The total gamma-ray flux per steradian expected from a particular point in the sky may then be found as

$$\frac{d\mathcal{F}}{d\Omega}(E) = \int_0^{d_{\text{max}}} d'^2 [\mathcal{F}_{\text{smooth}}(d', E) + \mathcal{F}_{\text{cross}}(d', E)n(d') + \mathcal{F}_h(d', E)n(d')] dd', \quad (15)$$

where $n = f\rho_\chi/f_\chi M_h$ is the local number density of halos at distance d' along the line of sight, and d_{max} is evaluated at the virial radius of the Milky Way's DM halo, which we take as $R_{\text{vir}} = 360$ kpc.

Statistical Analysis. — To determine the substructure properties required to explain the *Fermi* excess, we express the gamma-ray flux in terms of the parameters of the annihilation and subhalo structure models described in the previous sections. We constrain these quantities using summary statistics of both the morphology of the gamma-ray excess and the photon arrival directions. We assume 100% annihilation of an $m_\chi = 100$ GeV DM particle into $b\bar{b}$ final states, and allow the overall annihilation cross-section $\langle \sigma v \rangle$ to float. This model does give a reasonable fit to the observed spectrum of the excess, but

because we do not perform a spectral fit to the gamma-ray data, in reality the assumed DM model has minimal impact on our results.

To constrain the morphological properties of the excess, we use the results of the analysis of the Galactic Center gamma-ray signal by [14]. We fit to the observed excess flux (differential in energy, measured at 2 GeV) integrated within each of the 9 innermost regions of interest (ROI), neglecting the outermost region due to its overlap with the *Fermi* bubbles. We approximate the reported values and errors for these regions as Gaussian. These 9 regions encapsulate the morphology of the excess flux for regions both above and below the Galactic Plane. We compare these to the modeled flux by integrating Eq. (15) over each ROI for a given substructure model and set of model parameters (f , M_h , $\langle \sigma v \rangle$ and γ). Note that γ here is the slope parameter of the Milky Way halo, not of the minihalos. We leave γ as a free parameter in each of our fits, assuming a fixed minihalo slope, α — and then carry out multiple fits, each with a different value for α . We approximate the morphology likelihood as a Gaussian, given by

$$\mathcal{L}_{\text{morph}} = \prod_{i=1}^9 \exp \left[-\frac{(\mathcal{F}_i - \mu_i)^2}{2\sigma_i^2} \right], \quad (16)$$

where i is the ROI index, μ_i is the mean flux at 2 GeV estimated by Calore *et al.* [14], \mathcal{F}_i is the corresponding prediction from Eq. (15), and σ_i is the sum in quadrature of the (correlated) systematic and (uncorrelated) statis-

tical error. Note that we neglect the correlations between systematic errors in different ROIs; this is a conservative choice, as it reduces our ability to rule out substructure models.

Statistical studies of the *Fermi* photon map have suggested that $\gtrsim 95\%$ of the excess originates from a population of unresolved point sources. Here we assume that any unresolved point-like emission comes from small-scale DM substructures. To include this in our analysis, we use the results from Lee *et al.* [16]. Their so-called ‘non-Poissonian template fit’ differentiates between Poissonian and non-Poissonian photon statistics, in order to distinguish between diffuse and point-like emission. We take the posterior distributions for the total flux from the point-like component ($I_{\text{PS}}^{\text{NFW}}$) and smooth component (I_{NFW}) from the region within 10° of the GC, with $|b| \geq 2^\circ$. To avoid using the data twice (i.e., the information from the total flux is already included in the morphology likelihood) we use only the posterior for their ratio (with 3FGL sources masked), $z \equiv x/y \equiv I_{\text{NFW}}/I_{\text{PS}}^{\text{NFW}}$. The posterior for the ratio is given by [34]

$$P(z|d) = \int_{-\infty}^{\infty} |y| P(zy, y|d) dy, \quad (17)$$

where $P(x, y|d)$ is the 2D joint posterior of the smooth and point-like fluxes, given *Fermi* data d . Given that the posteriors for I_{NFW} and $I_{\text{PS}}^{\text{NFW}}$ are uncorrelated in the results of [16], we construct the joint distribution $P(x, y|d)$ from the individual 1D distributions in Fig. S4 of that paper. We reinterpret this posterior as a likelihood function and denote it $\mathcal{L}_{\text{PS}}(z)$, and we use $z = \mathcal{F}_{\text{smooth}}/(\mathcal{F}_{\text{h}} + \mathcal{F}_{\text{cross}})$, where \mathcal{F} is the total flux predicted within the Lee *et al.* ROI ($r \leq 10^\circ$, $|b| \geq 2^\circ$) according to Eq. (15).

The joint posterior for the parameters of our model, Θ , is given by (up to an irrelevant normalization constant)

$$P(\Theta|d) \propto \mathcal{L}_{\text{PS}} \mathcal{L}_{\text{morph}} P(\Theta) \quad (18)$$

where $P(\Theta) = P(\gamma)P(M_h)P(\langle\sigma v\rangle)P(f)$ is the prior distribution for the parameters. We adopt uniform priors on $\gamma \in [0, 3]$, $f \in [0, 1]$, $\log_{10}(M_h/M_\odot) \in [-12, 9]$ and $\log_{10}(\langle\sigma v\rangle/\text{cm}^3 \text{s}^{-1}) \in [-40, -20]$. We use a nested sampling procedure to sample from the posterior distribution and infer the parameters of substructure models.

Substructure as the source of the excess. — Taking the substructure to consist of NFW subhalos, we performed scans for three different choices of the subhalo inner slope, α . We show the flux profiles for the resulting posterior mean values of the parameters in Fig. 1.

While the subhalo models all provide reasonable morphological fits (reduced χ^2 values from 0.24 to 1.0), this requires a substantial abundance of substructure in the GC if the point source population of [16] is to be attributed to DM halos. In Fig. 2, we show 95% (highest

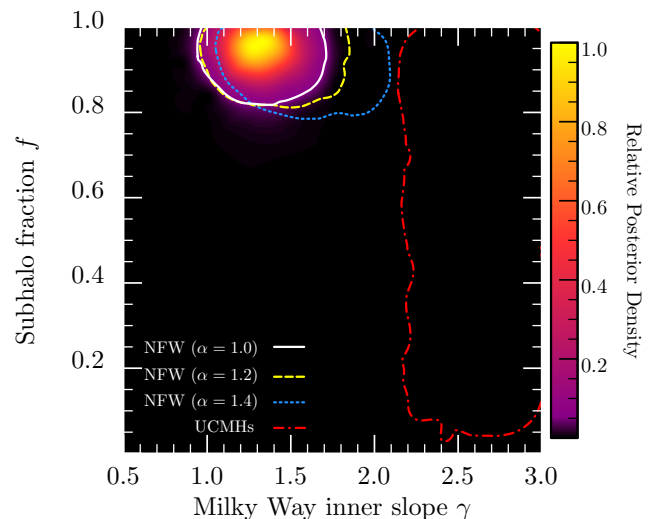


FIG. 2. Posterior probability densities and 95% confidence level credible regions for the substructure fraction and the inner slope of the Milky Way’s DM density profile, for four different substructure models. Shading corresponds to the posterior density for the the non-contracted NFW profile ($\alpha = 1.0$).

posterior density) credible regions for γ and f , marginalizing over both M_h and $\langle\sigma v\rangle$. For all three choices of α , we find $f \gtrsim 0.8$. Given the relatively small scale of the Galactic Center, any substructure present within this region would be expected to undergo mergers, stellar encounters, and tidal disruptions. According to both analytical and numerical studies [17, 23, 35–39], the net effect of these interactions would be the destruction of the majority of halos, and a decreased amount of substructure at small Galactic radii. Estimates of the substructure fraction within 3 kpc of the GC vary, but all studies with sufficient resolution predict $f \lesssim 0.05$. Given the difference between this value of f and the much larger value required to explain the *Fermi* excess, we conclude that the Galactic Center point source population is not constituted in any significant way by NFW subhalos.

UCMHs can be strong sources of DM annihilation, so one might expect that a smaller number of UCMHs would produce the same signal as a greater number of NFW subhalos. We show the resulting 95% confidence credible regions on γ and f for UCMH substructure in Fig. 2, marginalized over both M_h and $\langle\sigma v\rangle$. Although it is possible to fit the data with a far lower substructure fraction, a large increase in the inner slope of the halo of the Milky Way is needed to explain the excess. This may be understood by considering that the annihilation rate per unit volume within a smooth halo ($f = 0$) will be $\mathcal{A} \propto \rho_\chi^2 \propto r^{2\gamma}$, while that in a clumpy halo ($f = 1$) goes as the number density of subhalos, $\mathcal{A} \propto \Gamma \rho_\chi \propto r^\gamma$, where Γ is the flux emitted per subhalo. This means that if the DM halo consists predominantly of substructure,

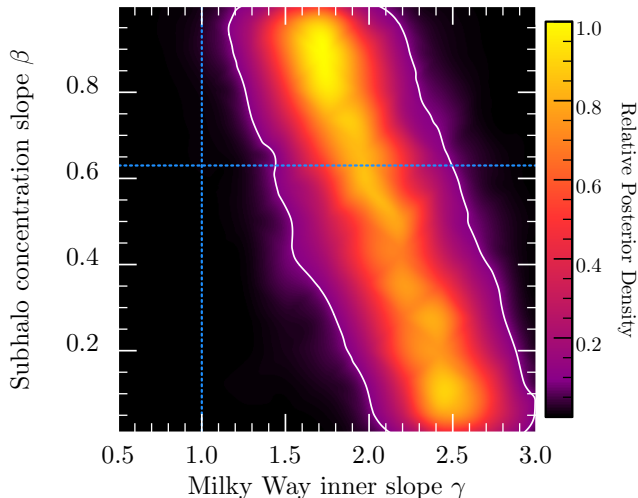


FIG. 3. Posterior probability density and 95% credible region for the radial slope of the subhalo concentration function and the inner slope of the Milky Way’s DM density profile. Vertical and horizontal dashed lines correspond to the results of the Aquarius simulations ($\gamma = 1$, $\beta = 0.63$; [17]).

the gamma-ray excess would be much flatter toward the Galactic Center than is observed, unless the Milky Way halo is significantly adiabatically contracted [40].

The model that we have considered so far assumes that subhalos look the same, and constitute the same fraction of DM, throughout the Galaxy. Although an increase in f or M_h toward the Galactic Center seems unlikely due to interactions of the halos with both baryonic and DM clumps, these same interactions strip the exterior regions of subhalos, resulting in an increased subhalo concentration parameter (c_{200}) closer to the GC. This increased concentration could allow NFW subhalos to provide annihilation at an increased rate, and thus lower the required value of f .

We investigated the effect of a spatially-varying subhalo concentration, modeled as a simple radial power law

$$\delta_c = Ar^{-\beta}, \quad (19)$$

with c_{200} determined from Eq. (3). Adopting a subhalo inner slope of $\alpha = 1.0$, a uniform prior on $\beta \in [0, 1]$ and $\log_{10} A \in [5, 10]$, we find that the case of a regular NFW Milky Way halo with zero adiabatic contraction ($\gamma = 1.0$) is excluded with more than 99% probability for all power law slopes $\beta < 1$. Within the Aquarius N-body simulation, it has been seen that subhalos follow Eq. (19) with a slope of $\beta \sim 0.63$ down to a resolution of ~ 10 kpc. At this value of β , even contracted NFW profiles right up to $\gamma = 1.4$ are excluded with more than 95% probability. Given the implausibility of the Milky Way halo having $\gamma > 1.4$, it therefore appears that even with a radially-varying subhalo concentration, DM anni-

hilation in subhalos is not compatible with the observed properties of the *Fermi* excess.

Summary & Conclusions.— Recent results suggest that the gamma-ray excess at the Galactic Center is produced by a population of unresolved point sources. We have investigated the idea that these point sources are small-scale DM substructures, using data on the morphology of the *Fermi-LAT* excess, as well as the statistics of individual photon arrivals.

We found that while the morphological properties of the excess can be explained by a substructure population, a significant amount of substructure is required. For a population of uncontracted NFW subhalos, we found that $\gtrsim 80\%$ of the Milky Way halo must exist as substructure, in stark contradiction with expectations from numerical simulations.

This implausibly large substructure fraction can be circumvented if the subhalos are extremely dense, as is the case for UCMHs. These are very strong producers of annihilation products, allowing a substructure fraction as low as $f \sim 0.05$. However, this requires a substantially contracted Milky Way inner slope of $\gamma \gtrsim 2.2$. Even if we allow the concentration of substructure to vary with distance from the GC, it is not possible to fit the properties of the observed excess with substructure unless $\gamma \gtrsim 1.4$. Given that such an extreme level of contraction is not borne out in numerical simulations, we conclude that the point sources detected via the wavelet analysis of Bartels *et al.* [15] and the non-Poissonian template fit of Lee *et al.* [16] are of astrophysical origin.

This paper has made use of MultiNest [41–43] and *pippi* [44]. HAC acknowledges the Australian Postgraduate Awards (APA). PS and RT are supported by STFC (ST/K00414X/1 and ST/N000838/1), and RT by an EPSRC Pathways to Impact grant. We acknowledge the University of Sydney HPC service for providing computational resources that have contributed to the research results reported in this paper.

* hamish.clark@sydney.edu.au

- [1] M. Ajello *et al.* (Fermi-LAT), *ApJ* **819**, 44 (2016), arXiv:1511.02938 [astro-ph.HE].
- [2] K. N. Abazajian and M. Kaplinghat, *Phys. Rev. D* **86**, 083511 (2012), arXiv:1207.6047 [astro-ph.HE].
- [3] O. Macias and C. Gordon, *Phys. Rev. D* **89**, 063515 (2014), arXiv:1312.6671 [astro-ph.HE].
- [4] T. Daylan, D. P. Finkbeiner, D. Hooper, T. Linden, S. K. N. Portillo, N. L. Rodd, and T. R. Slatyer, *Physics of the Dark Universe* **12**, 1 (2016), arXiv:1402.6703 [astro-ph.HE].
- [5] E. Carlson and S. Profumo, *Phys. Rev. D* **90**, 023015 (2014), arXiv:1405.7685 [astro-ph.HE].
- [6] J. Petrović, P. Dario Serpico, and G. Zaharijaš, *JCAP* **10**, 052 (2014), arXiv:1405.7928 [astro-ph.HE].
- [7] D. Gaggero, M. Taoso, A. Urbano, M. Valli, and P. Ullio,

- JCAP **12**, 056 (2015), arXiv:1507.06129 [astro-ph.HE].
- [8] K. N. Abazajian, JCAP **3**, 010 (2011), arXiv:1011.4275 [astro-ph.HE].
- [9] K. N. Abazajian, N. Canac, S. Horiuchi, and M. Kaplinghat, Phys. Rev. D **90**, 023526 (2014), arXiv:1402.4090 [astro-ph.HE].
- [10] N. Mirabal, MNRAS **436**, 2461 (2013), arXiv:1309.3428 [astro-ph.HE].
- [11] D. Hooper and L. Goodenough, Physics Letters B **697**, 412 (2011), arXiv:1010.2752 [hep-ph].
- [12] D. Hooper and T. Linden, Phys. Rev. D **84**, 123005 (2011), arXiv:1110.0006 [astro-ph.HE].
- [13] F. Calore, I. Cholis, C. McCabe, and C. Weniger, Phys. Rev. D **91**, 063003 (2015), arXiv:1411.4647 [hep-ph].
- [14] F. Calore, I. Cholis, and C. Weniger, JCAP **3**, 038 (2015), arXiv:1409.0042.
- [15] R. Bartels, S. Krishnamurthy, and C. Weniger, Physical Review Letters **116**, 051102 (2016), arXiv:1506.05104 [astro-ph.HE].
- [16] S. K. Lee, M. Lisanti, B. R. Safdi, T. R. Slatyer, and W. Xue, Physical Review Letters **116**, 051103 (2016), arXiv:1506.05124 [astro-ph.HE].
- [17] V. Springel, J. Wang, M. Vogelsberger, A. Ludlow, A. Jenkins, A. Helmi, J. F. Navarro, C. S. Frenk, and S. D. M. White, MNRAS **391**, 1685 (2008), arXiv:0809.0898.
- [18] M. Kamionkowski, S. M. Koushiappas, and M. Kuhlen, Phys. Rev. D **81**, 043532 (2010), arXiv:1001.3144 [astro-ph.GA].
- [19] D. Anderhalden and J. Diemand, JCAP **4**, 009 (2013), arXiv:1302.0003.
- [20] R. Bartels and S. Ando, Phys. Rev. D **92**, 123508 (2015), arXiv:1507.08656.
- [21] J. F. Navarro, C. S. Frenk, and S. D. M. White, ApJ **462**, 563 (1996), astro-ph/9508025.
- [22] J. S. B. Wyithe, E. L. Turner, and D. N. Spergel, ApJ **555**, 504 (2001), astro-ph/0007354.
- [23] F. Jiang and F. C. van den Bosch, ArXiv e-prints (2016), arXiv:1610.02399.
- [24] K. T. E. Chua, A. Pillepich, V. Rodriguez-Gomez, M. Vogelsberger, S. Bird, and L. Hernquist, ArXiv e-prints (2016), arXiv:1611.07991.
- [25] C. A. Correa, J. S. B. Wyithe, J. Schaye, and A. R. Duffy, MNRAS **452**, 1217 (2015), arXiv:1502.00391.
- [26] M. Ricotti and A. Gould, ApJ **707**, 979 (2009), arXiv:0908.0735.
- [27] P. Scott and S. Sivertsson, Phys. Rev. Lett. **103**, 211301 (2009), arXiv:0908.4082.
- [28] V. S. Berezhinsky, V. I. Dokuchaev, and Y. N. Eroshenko, Gravitation and Cosmology **18**, 57 (2012).
- [29] V. S. Berezhinsky, V. I. Dokuchaev, and Y. N. Eroshenko, JCAP **11**, 059 (2013), arXiv:1308.6742 [astro-ph.CO].
- [30] A. S. Josan and A. M. Green, Phys. Rev. D **82**, 083527 (2010), arXiv:1006.4970 [astro-ph.CO].
- [31] T. Bringmann, P. Scott, and Y. Akrami, Phys. Rev. D **85**, 125027 (2012), arXiv:1110.2484 [astro-ph.CO].
- [32] S. Shandera, A. L. Erickcek, P. Scott, and J. Y. Galarza, Phys. Rev. D **88**, 103506 (2013), arXiv:1211.7361 [astro-ph.CO].
- [33] G. Aslanyan, L. C. Price, J. Adams, T. Bringmann, H. A. Clark, R. Easther, G. F. Lewis, and P. Scott, Phys. Rev. Lett. **117**, 141102 (2016), arXiv:1512.04597.
- [34] J. H. Curtiss, The Annals of Mathematical Statistics **12**, 409 (1941).
- [35] J. Diemand, M. Kuhlen, and P. Madau, ApJ **667**, 859 (2007), astro-ph/0703337.
- [36] J. Diemand, M. Kuhlen, and P. Madau, ApJ **679**, 1680-1683 (2008).
- [37] J. Diemand, M. Kuhlen, P. Madau, M. Zemp, B. Moore, D. Potter, and J. Stadel, Nature **454**, 735 (2008), arXiv:0805.1244.
- [38] Q. Zhu, F. Marinacci, M. Maji, Y. Li, V. Springel, and L. Hernquist, MNRAS **458**, 1559 (2016), arXiv:1506.05537.
- [39] M. Stref and J. Lavalley, ArXiv e-prints (2016), arXiv:1610.02233.
- [40] Note that this is not an effect of favoring any particular value of M_h , as the substructure boost factor due to UCMHs is in fact independent of their mass function [45].
- [41] F. Feroz and M. P. Hobson, MNRAS **384**, 449 (2008), arXiv:0704.3704.
- [42] F. Feroz, M. P. Hobson, and M. Bridges, MNRAS **398**, 1601 (2009), arXiv:0809.3437.
- [43] F. Feroz, M. P. Hobson, E. Cameron, and A. N. Pettitt, ArXiv e-prints (2013), arXiv:1306.2144 [astro-ph.IM].
- [44] P. Scott, Eur. Phys. J. Plus **127**, 138 (2012), arXiv:1206.2245.
- [45] H. A. Clark, N. Iwanus, P. J. Elahi, G. F. Lewis, and P. Scott, ArXiv e-prints (2016), arXiv:1611.08619.